Measurement of D^0–$\bar{D}^0$ mixing and search for CP violation in $D^0 \to K^+K^-, \pi^+\pi^-$ decays with the full Belle data set

Belle Collaboration

M. Starič [w,*], A. Abdesselam [be], I. Adachi [n,k], H. Aihara [bk], K. Arinstein [d,av], D.M. Asner [ax], T. Aushev [al,v], R. Ayad [be], T. Aziz [bf], V. Babu [bf], I. Badhrees [be,aa], S. Bahinipati [p], A.M. Bakich [bd], V. Bansal [ax], J. Biswal [w], A. Bondar [d,av], G. Bonvicini [bp], A. Bozek [as], M. Bračko [ah,w], T.E. Browder [m], D. Červenkov [e], V. Chekelian [ai], A. Chen [ap], B.G. Cheon [l], K. Chilikin [v], R. Chistov [v], K. Cho [ab], V. Chobanova [ai], Y. Choi [bc], D. Cinabro [bp], J. Dalseno [ai,bg], M. Danilov [v,ak], Z. Doležal [e], D. Dutta [bf], S. Eidelman [d,av], D. Epifanov [bk], H. Farhat [bp], J.E. Fast [ax], T. Ferber [h], B.G. Fulsom [ax], V. Gaur [bf], N. Gabyshev [d,av], S. Ganguly [bp], A. Garmash [d,av], R. Gillard [bp], R. Glattauer [t], Y.M. Goh [l], P. Goldenzweig [y], B. Golob [af,w], J. Grygier [y], J. Haba [n,k], T. Hara [n,k], K. Hayasaka [an], H. Hayashii [ao], X.H. He [ay], W.-S. Hou [ar], C.-L. Hsu [aj], T. Iijima [an,am], K. Inami [am], G. Inguglia [h], A. Ishikawa [bi], R. Itoh [n,k], I. Jaegle [m], D. Joffe [z], T. Julius [aj], K.H. Kang [ad], T. Kawasaki [at], T. Keck [y], C. Kiesling [ai], D.Y. Kim [bb], J.B. Kim [ac], J.H. Kim [ab], M.J. Kim [ad], S.H. Kim [l], Y.J. Kim [ab], K. Kinoshita [g], B.R. Ko [ac], P. Kodyš [e], S. Korpar [ah,w], P. Križan [af,w], P. Krokovny [d,av], T. Kumita [bm], A. Kuzmin [d,av], Y.-J. Kwon [br], J.S. Lange [i], I.S. Lee [l], P. Lewis [m], Y. Li [bo], L. Li Gioi [ai], J. Libby [q], D. Liventsev [bo,n], P. Lukin [d,av], M. Masuda [bj], D. Matvienko [d,av], K. Miyabayashi [ao], H. Miyata [at], R. Mizuk [v,ak], G.B. Mohanty [bf], A. Moll [ai,bg], H.K. Moon [ac], R. Mussa [u], M. Nakao [n,k], T. Nanut [w], Z. Natkaniec [as], N.K. Nisar [bf], S. Nishida [n,k], S. Ogawa [bh], S. Okuno [x], P. Pakhlov [v,ak], G. Pakhlova [al,v], B. Pal [g], C.W. Park [bc], H. Park [ad], T.K. Pedlar [ag], L. Pesántez [c], R. Pestotnik [w], M. Petrič [w], L.E. Piilonen [bo], E. Ribežl [w], M. Ritter [ai], A. Rostomyan [h], Y. Sakai [n,k], S. Sandilya [bf], T. Sanuki [bi], V. Savinov [az], O. Schneider [ae], G. Schnell [a,o], C. Schwanda [t], A.J. Schwartz [g], K. Senyo [bq], V. Shebalin [d,av], C.P. Shen [b], T.-A. Shibata [bl], J.-G. Shiu [ar], B. Shwartz [d,av], F. Simon [ai,bg], Y.-S. Sohn [br], A. Sokolov [s], E. Solovieva [v], S. Stanič [au], M. Steder [h], M. Sumihama [j], U. Tamponi [u,bn], Y. Teramoto [aw], K. Trabelsi [n,k], M. Uchida [bl], S. Uehara [n,k], T. Uglov [v,al], Y. Unno [l], S. Uno [n,k], P. Urquijo [aj], Y. Usov [d,av], C. Van Hulse [a], P. Vanhoefer [ai], G. Varner [m], A. Vinokurova [d,av], V. Vorobyev [d,av], M.N. Wagner [i], C.H. Wang [aq], M.-Z. Wang [ar], P. Wang [r], X.L. Wang [bo], M. Watanabe [at], Y. Watanabe [x], K.M. Williams [bo], E. Won [ac], S. Yashchenko [h], Y. Yook [br], C.Z. Yuan [r], Z.P. Zhang [ba], V. Zhilich [d,av], V. Zhulanov [d,av], M. Ziegler [y], A. Zupanc [w]

[a] *University of the Basque Country UPV/EHU, 48080 Bilbao, Spain*
[b] *Beihang University, Beijing 100191, PR China*
[c] *University of Bonn, 53115 Bonn, Germany*
[d] *Budker Institute of Nuclear Physics SB RAS, Novosibirsk 630090, Russian Federation*
[e] *Faculty of Mathematics and Physics, Charles University, 121 16 Prague, Czech Republic*
[f] *Chiba University, Chiba 263-8522, Japan*
[g] *University of Cincinnati, Cincinnati, OH 45221, USA*

[h] *Deutsches Elektronen–Synchrotron, 22607 Hamburg, Germany*
[i] *Justus-Liebig-Universität Gießen, 35392 Gießen, Germany*
[j] *Gifu University, Gifu 501-1193, Japan*
[k] *SOKENDAI (The Graduate University for Advanced Studies), Hayama 240-0193, Japan*
[l] *Hanyang University, Seoul 133-791, South Korea*
[m] *University of Hawaii, Honolulu, HI 96822, USA*
[n] *High Energy Accelerator Research Organization (KEK), Tsukuba 305-0801, Japan*
[o] *IKERBASQUE, Basque Foundation for Science, 48013 Bilbao, Spain*
[p] *Indian Institute of Technology Bhubaneswar, Satya Nagar 751007, India*
[q] *Indian Institute of Technology Madras, Chennai 600036, India*
[r] *Institute of High Energy Physics, Chinese Academy of Sciences, Beijing 100049, PR China*
[s] *Institute for High Energy Physics, Protvino 142281, Russian Federation*
[t] *Institute of High Energy Physics, Vienna 1050, Austria*
[u] *INFN – Sezione di Torino, 10125 Torino, Italy*
[v] *Institute for Theoretical and Experimental Physics, Moscow 117218, Russian Federation*
[w] *J. Stefan Institute, 1000 Ljubljana, Slovenia*
[x] *Kanagawa University, Yokohama 221-8686, Japan*
[y] *Institut für Experimentelle Kernphysik, Karlsruher Institut für Technologie, 76131 Karlsruhe, Germany*
[z] *Kennesaw State University, Kennesaw GA 30144, USA*
[aa] *King Abdulaziz City for Science and Technology, Riyadh 11442, Saudi Arabia*
[ab] *Korea Institute of Science and Technology Information, Daejeon 305-806, South Korea*
[ac] *Korea University, Seoul 136-713, South Korea*
[ad] *Kyungpook National University, Daegu 702-701, South Korea*
[ae] *École Polytechnique Fédérale de Lausanne (EPFL), Lausanne 1015, Switzerland*
[af] *Faculty of Mathematics and Physics, University of Ljubljana, 1000 Ljubljana, Slovenia*
[ag] *Luther College, Decorah, IA 52101, USA*
[ah] *University of Maribor, 2000 Maribor, Slovenia*
[ai] *Max-Planck-Institut für Physik, 80805 München, Germany*
[aj] *School of Physics, University of Melbourne, Victoria 3010, Australia*
[ak] *Moscow Physical Engineering Institute, Moscow 115409, Russian Federation*
[al] *Moscow Institute of Physics and Technology, Moscow Region 141700, Russian Federation*
[am] *Graduate School of Science, Nagoya University, Nagoya 464-8602, Japan*
[an] *Kobayashi–Maskawa Institute, Nagoya University, Nagoya 464-8602, Japan*
[ao] *Nara Women's University, Nara 630-8506, Japan*
[ap] *National Central University, Chung-li 32054, Taiwan*
[aq] *National United University, Miao Li 36003, Taiwan*
[ar] *Department of Physics, National Taiwan University, Taipei 10617, Taiwan*
[as] *H. Niewodniczanski Institute of Nuclear Physics, Krakow 31-342, Poland*
[at] *Niigata University, Niigata 950-2181, Japan*
[au] *University of Nova Gorica, 5000 Nova Gorica, Slovenia*
[av] *Novosibirsk State University, Novosibirsk 630090, Russian Federation*
[aw] *Osaka City University, Osaka 558-8585, Japan*
[ax] *Pacific Northwest National Laboratory, Richland, WA 99352, USA*
[ay] *Peking University, Beijing 100871, PR China*
[az] *University of Pittsburgh, Pittsburgh, PA 15260, USA*
[ba] *University of Science and Technology of China, Hefei 230026, PR China*
[bb] *Soongsil University, Seoul 156-743, South Korea*
[bc] *Sungkyunkwan University, Suwon 440-746, South Korea*
[bd] *School of Physics, University of Sydney, NSW 2006, Australia*
[be] *Department of Physics, Faculty of Science, University of Tabuk, Tabuk 71451, Saudi Arabia*
[bf] *Tata Institute of Fundamental Research, Mumbai 400005, India*
[bg] *Excellence Cluster Universe, Technische Universität München, 85748 Garching, Germany*
[bh] *Toho University, Funabashi 274-8510, Japan*
[bi] *Tohoku University, Sendai 980-8578, Japan*
[bj] *Earthquake Research Institute, University of Tokyo, Tokyo 113-0032, Japan*
[bk] *Department of Physics, University of Tokyo, Tokyo 113-0033, Japan*
[bl] *Tokyo Institute of Technology, Tokyo 152-8550, Japan*
[bm] *Tokyo Metropolitan University, Tokyo 192-0397, Japan*
[bn] *University of Torino, 10124 Torino, Italy*
[bo] *CNP, Virginia Polytechnic Institute and State University, Blacksburg, VA 24061, USA*
[bp] *Wayne State University, Detroit, MI 48202, USA*
[bq] *Yamagata University, Yamagata 990-8560, Japan*
[br] *Yonsei University, Seoul 120-749, South Korea*

A R T I C L E   I N F O

A B S T R A C T

We report an improved measurement of D^0–$\overline{D}^0$ mixing and a search for *CP* violation in D^0 decays to *CP*-even final states K^+K^- and $\pi^+\pi^-$. The measurement is based on the final Belle data sample of 976 fb^{-1}. The results are $y_{CP} = (1.11 \pm 0.22 \pm 0.09)\%$ and $A_\Gamma = (-0.03 \pm 0.20 \pm 0.07)\%$, where the first uncertainty is statistical and the second is systematic.

1. Introduction

Mixing of neutral mesons originates from a difference between mass and flavor eigenstates of the meson–antimeson system. For D^0 mesons, the mass eigenstates are usually expressed as $|D^0_{1,2}\rangle = p|D^0\rangle \pm q|\overline{D}^0\rangle$ (the sum for D^0_1 and the difference for D^0_2), with $|p|^2 + |q|^2 = 1$. The D^0–$\overline{D}^0$ mixing rate is characterized by two parameters: $x = \Delta m/\Gamma$ and $y = \Delta\Gamma/2\Gamma$, where $\Delta m = m_2 - m_1$ and $\Delta\Gamma = \Gamma_2 - \Gamma_1$ are the differences in mass and decay width, respectively, between the mass eigenstates D^0_2 and D^0_1, and Γ is the average D^0 decay width. If $p = q$, the mass eigenstates are also CP eigenstates; otherwise, $D^0_{1,2}$ are not CP eigenstates and CP violation arises in decays of D^0 mesons [1].

Mixing in D^0 decays to CP eigenstates, such as $D^0 \to K^+K^-$, gives rise to an effective lifetime τ that differs from that in decays to flavor eigenstates such as $D^0 \to K^-\pi^+$ [2]. The observable

$$y_{CP} = \frac{\tau(D^0 \to K^-\pi^+)}{\tau(D^0 \to K^+K^-)} - 1 \qquad (1)$$

is equal to the mixing parameter y if CP is conserved.[1] Otherwise, the effective lifetimes of D^0 and $\overline{D}^0$ decaying to the same CP eigenstate differ and the asymmetry

$$A_\Gamma = \frac{\tau(\overline{D}^0 \to K^-K^+) - \tau(D^0 \to K^+K^-)}{\tau(\overline{D}^0 \to K^-K^+) + \tau(D^0 \to K^+K^-)} \qquad (2)$$

is non-zero. The observables y_{CP} and A_Γ are, in the absence of direct CP violation, related to the mixing parameters x and y as [2,3] $y_{CP} = \frac{1}{2}(|q/p| + |p/q|)y\cos\phi - \frac{1}{2}(|q/p| - |p/q|)x\sin\phi$ and $A_\Gamma = \frac{1}{2}(|q/p| - |p/q|)y\cos\phi - \frac{1}{2}(|q/p| + |p/q|)x\sin\phi$, where $\phi = \arg(q/p)$.

The first evidence for D^0–$\overline{D}^0$ mixing was obtained in 2007 by Belle using $D^0 \to K^+K^-$ and $D^0 \to \pi^+\pi^-$ [4] and by BaBar using "wrong-sign" $D^0 \to K^+\pi^-$ decays [5]. These results were later confirmed with high precision by LHCb [6] and CDF [7]. The asymmetry A_Γ has been measured by Belle [4], BaBar [8], CDF [9] and LHCb [10,11]. The measurements of y_{CP} have been reported also by BaBar [8], LHCb [12] and BESIII [13]. Here, we report a new measurement of $D^0 \to K^+K^-, \pi^+\pi^-$ decays using almost twice as much data as in Ref. [4] and an improved analysis method. The resolution function now accounts for a dependence upon polar angle and different configurations of the silicon vertex detector (see below).

2. Event selection

The measurement is based on the final data set of 976 fb^{-1} recorded by the Belle detector [14] at the KEKB asymmetric-energy e^+e^- collider [15], which operated primarily at the center-of-mass energy of the $\Upsilon(4S)$ resonance, and 60 MeV below. A fraction of the data was recorded at the $\Upsilon(1S)$, $\Upsilon(2S)$, $\Upsilon(3S)$, and $\Upsilon(5S)$ resonances; these data are included in the measurement. The Belle detector is described in detail elsewhere [14]. It includes a silicon vertex detector (SVD), a central drift chamber (CDC), an array of aerogel Cherenkov counters, and time-of-flight scintillation counters. Two different SVD configurations were used: a 3-layer configuration for the first 153 fb^{-1} of data and a 4-layer configuration [16] for the remaining 823 fb^{-1} of data.

The decays $D^0 \to K^+K^-$, $D^0 \to \pi^+\pi^-$ and $D^0 \to K^-\pi^+$ are reconstructed in the decay chain $D^{*+} \to D^0\pi^+$, where the charge of the D^*-daughter pion (which has low momentum and thus is

referred to as "slow") is used to tag the initial flavor of the D^0 meson.[2] Each final-state charged particle is required to have at least two associated SVD hits in each of the longitudinal and azimuthal measuring coordinates. To select pion and kaon candidates, we impose particle identification criteria based on energy deposition in the CDC, the track time of flight, and information from the aerogel Cherenkov counters [17]. The identification efficiencies and the misidentification probabilities are about 85% and 9%, respectively, for the D^0 daughters, and about 99% and 2%, respectively, for the slow pion from D^{*+} decay. The D^0 daughters are refitted to a common vertex. The D^0 production vertex is determined as the intersection of the D^0 trajectory with that of the slow pion, subject to the constraint that they both originate from the e^+e^- interaction region. Confidence levels exceeding 10^{-3} are required for both fits. To reject D mesons produced in B-meson decays and also to suppress combinatorial background, the D^{*+} momentum in the e^+e^- center-of-mass system (CMS) is required to satisfy $p_D^* > 2.5$ GeV/c for the data taken below the $\Upsilon(5S)$ resonance and $p_D^* > 3.1$ GeV/c for the $\Upsilon(5S)$ data.

We select D^0 candidates using two kinematic variables: the invariant mass M of the D^0 and the energy released in the D^{*+} decay $q = (M_{D^*} - M - m_\pi)c^2$, where M_{D^*} is the invariant mass of the D^{*+} decay products and m_π is the mass of the charged pion. The proper decay time of the D^0 candidate is calculated from the projection of the vector joining the two vertices, $\vec{L}$, onto the D^0 momentum vector $\vec{p}$: $t = m_{D^0}\vec{L} \cdot \vec{p}/p^2$, where m_{D^0} is the nominal D^0 mass [18]. The proper decay time uncertainty σ_t of the candidate D^0 is evaluated from the error matrices of the production and decay vertices.

The samples of events for the lifetime measurements are selected using variables $\Delta M \equiv M - m_{D^0}$, $\Delta q = q - q_0$, and σ_t, where q_0 is the nominal energy released in the D^{*+} decay (5.86 MeV). These selection criteria are optimized using Monte Carlo (MC) simulation by minimizing the statistical uncertainty on y_{CP}. The simulation is based on EvtGen [19] and Pythia generators [20]; simulated events were processed through a full Belle detector simulation using Geant 3 [21] and Fluka [22] to simulate hadronic interactions. The optimization gives the following selection criteria: $|\Delta M| < 2.25\sigma_M$ for all events, where σ_M is the r.m.s. width of the D^0 invariant mass peak; $|\Delta q| < 0.66$ MeV and $\sigma_t < 440$ fs for the 3-layer SVD configuration; and $|\Delta q| < 0.82$ MeV and $\sigma_t < 370$ fs for the 4-layer SVD configuration. The D^0 peak, shown in Fig. 1, is not purely Gaussian in shape. In addition, the width σ_M depends on the decay mode and on the SVD configuration. Typically $\sigma_M \approx 6$–8 MeV/c^2.

Background is estimated from sidebands in M. The sideband position is optimized using MC simulation in order to minimize systematic uncertainties arising from small differences between the decay time distribution of events in the sideband and that of background events in the signal region. The sideband windows are shown in Fig. 1. The yields of selected events are 242×10^3 K^+K^-, 114×10^3 $\pi^+\pi^-$, and 2.61×10^6 $K^-\pi^+$, with signal purities of 98.0%, 92.9% and 99.7%, respectively. The dominant background is combinatorial.

3. Lifetime fit

The measurement is performed by doing a simultaneous binned maximum likelihood fit to five data samples: $D^0 \to K^+K^-$, $\overline{D}^0 \to K^+K^-$, $D^0 \to \pi^+\pi^-$, $\overline{D}^0 \to \pi^+\pi^-$, and the sum of $D^0 \to K^-\pi^+$ and $\overline{D}^0 \to K^+\pi^-$. The proper decay time distribution is parameterized as

---

[1] Using phase convention $CP|D^0\rangle = -|\overline{D}^0\rangle$.

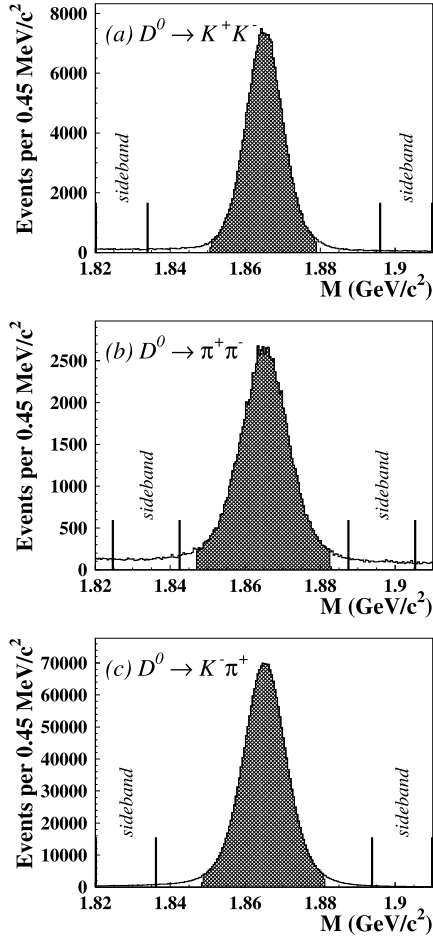[2] Throughout this paper, charge-conjugate modes are included implicitly unless noted otherwise.

Fig. 1. D^0 invariant mass distributions obtained with the 4-layer SVD configuration after applying optimized selection criteria on Δq and σ_t. (a) $D^0 \to K^+K^-$; (b) $D^0 \to \pi^+\pi^-$; and (c) $D^0 \to K^-\pi^+$. The shaded regions indicate events selected for the measurement. The sideband positions are also indicated.

$$F(t) = \frac{N}{\tau} \int_0^\infty e^{-t'/\tau} R(t - t')dt' + B(t), \qquad (3)$$

where τ is the effective lifetime, N is the signal yield, $R(t)$ is a resolution function, and $B(t)$ is the background contribution that is fixed from a fit to the sideband distribution. The decay time acceptance is studied with MC simulations and found to be constant to good precision within the selected range.

The construction of the resolution function is similar to that of our previous analysis [4] but improved to take into account a possible shape asymmetry and D^0 polar angle dependence. It is constructed using a normalized distribution of σ_t: for each σ_t bin, a common-mean double- or triple-Gaussian probability density function is constructed. The fractions w_k and widths σ_k^{pull} of these Gaussian distributions are obtained from fits to the MC distribution of pulls, defined as $(t - t_{\text{gen}})/\sigma_t$, where t and t_{gen} are the reconstructed and generated proper decay times, respectively, of simulated D^0 decays. The resolution function is

$$R(t) = \sum_{i=1}^n f_i \sum_{k=1}^{n_g} w_k G(t; \mu_i, \sigma_{ik}), \qquad (4)$$

where $G(t; \mu_i, \sigma_{ik})$ is a Gaussian distribution of mean μ_i and width σ_{ik}; f_i is the fraction of events in the i-th bin of the σ_t distribution; the index k runs over the number of Gaussians n_g
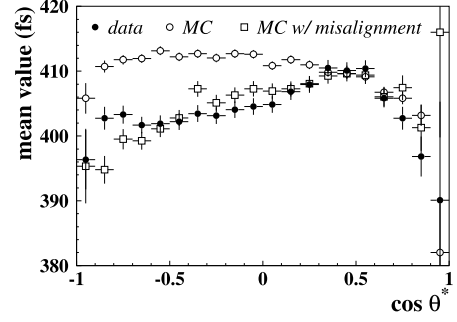

Fig. 2. Mean of the sideband-subtracted proper decay time distribution of $D^0 \to K^-\pi^+$ decays as a function of $\cos\theta^*$ for 4-layer SVD data (full circles) and corresponding MC simulation (open circles) and for one of the MC samples with misaligned SVD (open squares) that shows a dependence similar to data. Similar behavior is observed also for 3-layer SVD configuration.

used for bin i; and the index i runs over the number of σ_t bins. The means and widths of the Gaussians are parameterized as

$$\mu_i = t_0 + a(\sigma_i - \overline{\sigma_t}) \qquad \sigma_{ik} = s_k \sigma_k^{\text{pull}} \sigma_i, \qquad (5)$$

where t_0 is a resolution function offset, a is a parameter to model a possible asymmetry of the resolution function, σ_i is the bin central value, $\overline{\sigma_t}$ is the mean of the σ_t distribution, and s_k is a width-scaling factor. The parameters s_k, t_0 and a, in addition to N and τ, are free parameters in the fit. To construct $R(t)$ with Eq. (4), a sideband-subtracted σ_t distribution is used.

From studies of the proper decay time distribution of $D^0 \to K^-\pi^+$ decays, we observe a significant dependence of its mean value on $\cos\theta^*$ (see Fig. 2), where θ^* is the polar angle of D^0 in CMS with respect to the direction of e^+. From MC studies, we find that this effect is due to a small misalignment of the SVD detector. The effect can be corrected for when fitting for the lifetime by allowing the resolution function offset t_0 to vary with $\cos\theta^*$. We thus measure y_{CP} and A_Γ in bins of $\cos\theta^*$, with the resolution function calculated separately for each bin. An additional requirement $|\cos\theta^*| < 0.9$ is imposed to suppress events with large offsets (about 1% of events).

The background term in Eq. (3) is parameterized as the sum of a component with zero lifetime and a component with an effective lifetime τ_b:

$$B(t) = N_b \int_0^\infty [p\delta(t') + (1-p)\frac{1}{\tau_b} e^{-t'/\tau_b}]R_b(t - t')dt'. \qquad (6)$$

The resolution function $R_b(t)$ is also parameterized with Eq. (4) except that, for each σ_t bin, the function is taken to be symmetric ($a = 0$) and always composed of three Gaussians, with the second and third scaling factors being equal ($s_2 = s_3$). The σ_t distribution is taken from an M sideband. The fraction p of the zero-lifetime component is found to be $\cos\theta^*$-dependent; its value is fixed in each bin using MC simulation. The parameters t_0, s_1, s_2 and τ_b are determined separately for each decay mode and SVD configuration from a fit to sideband distributions summed over $\cos\theta^*$ bins. However, the background shape is still $\cos\theta^*$ dependent, because the σ_t distribution, the zero-lifetime fraction p and the yield N_b all depend on $\cos\theta^*$. The quality of these fits exceeds 15% confidence level (CL).

To extract y_{CP} and A_Γ, the decay modes are fitted simultaneously in each $\cos\theta^*$ bin and separately for each of the two SVD configurations. The parameters shared among the decay modes are y_{CP} and A_Γ (between KK and $\pi\pi$), t_0 and a (among all decay modes), and parameters s_1, s_2 and s_3, up to an overall scaling fac-
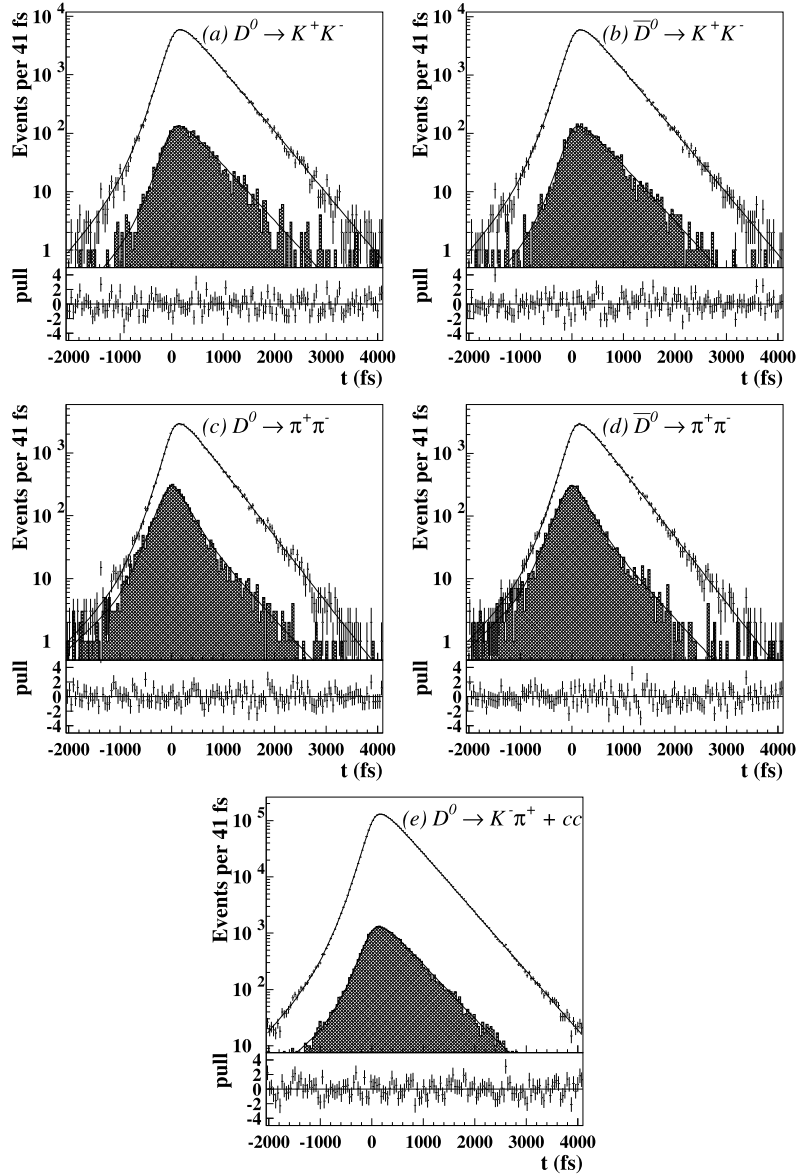
Fig. 3. Proper decay time distributions summed over $\cos\theta^*$ bins and both running periods with the sum of fitted functions superimposed. Shown as error bars are the distributions of events in the M signal region while the shaded area represents background contributions as obtained from M sidebands. The plots beneath the distributions show the pulls of simultaneous fit (i.e., residuals divided by errors).

tor. Results for individual $\cos\theta^*$ bins and for the two data sets are combined into an overall result via a least-squares fit to a constant.

The fitting procedure is tested with a generic MC sample equivalent to six times the data statistics. The fitted y_{CP} and A_Γ are consistent with the input zero value, and the fitted $K\pi$ lifetime is consistent with the generated value. Linearity tests performed with MC-simulated events re-weighted to reflect different y_{CP} and A_Γ values show no bias.

The fitting procedure is then applied to the measured data. The fitted proper decay time distributions summed over $\cos\theta^*$ bins and running periods with the two SVD configurations are shown in Fig. 3. The pulls, plotted beneath each fitted distribution, show no significant structure. The normalized χ^2 is 1.13.[3] The confidence levels of individual fits in bins of $\cos\theta^*$ are above 5%, except for one with CL = 3.3%, and are distributed uniformly.

The fitted values of y_{CP} and A_Γ in bins of $\cos\theta^*$ are shown in Figs. 4 and 5. The values obtained with a least-squares fit to a constant are $y_{CP} = (1.11 \pm 0.22)\%$ and $A_\Gamma = (-0.03 \pm 0.20)\%$, where the uncertainties are statistical only; the confidence levels are 32% and 40%, respectively. The fitted D^0 lifetime is (408.46 ± 0.54) fs (statistical uncertainty only), which is consistent with the current world average of (410.1 ± 1.5) fs [18].

4. Systematic uncertainties

The estimated systematic uncertainties are listed in Table 1. The impact of imperfect SVD alignment is studied with a dedicated signal MC simulation in which different local and global SVD misalignments are modeled. Local misalignment refers to a random translation and rotation of each individual silicon strip detector according to the alignment precision, while global misalignment refers to a translation and rotation of the entire SVD with respect to the CDC. The systematic uncertainties are taken to be the r.m.s.
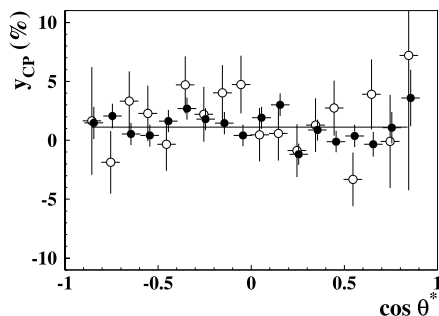
---

[3] We use Pearson's definition of χ^2 and take only the bins with the fitted function greater than one.

Fig. 4. Fitted y_{CP} in bins of $\cos\theta^*$ for 3-layer SVD data (open circles) and for 4-layer SVD data (full circles). The horizontal line is the result of fitting the points to a constant.
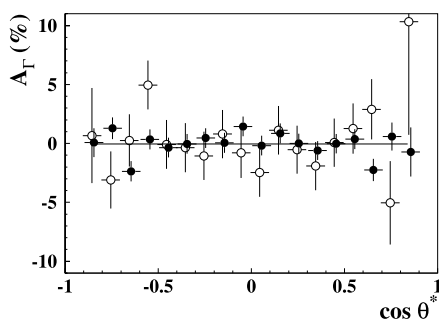

Fig. 5. Fitted A_Γ in bins of $\cos\theta^*$ for 3-layer SVD data (open circles) and for 4-layer SVD data (full circles). The horizontal line is the result of fitting the points to a constant.

Table 1
Systematic uncertainties.

Source	Δy_{CP} (%)	ΔA_Γ (%)
SVD misalignment	0.060	0.041
Mass window position	0.007	0.009
Background	0.059	0.050
Resolution function	0.030	0.002
Binning	0.021	0.010
Total	0.092	0.066

of the differences between these results and the nominal result that assumes perfect SVD alignment. We obtain 0.060% for y_{CP} and 0.041% for A_Γ.

The uncertainty due to the position of the mass window is estimated by varying the position of the window by the small differences found between MC simulation and data in the position of the D^0 mass peak, about ± 1 MeV/c^2. This resulting uncertainty is relatively small: 0.007% for y_{CP} and 0.009% for A_Γ.

Background contributes to the systematic uncertainty in two ways: statistical fluctuations of sideband distributions and modeling. The former is found to contribute 0.051% for y_{CP} and 0.050% for A_Γ. The latter arises from modeling the background distribution with that of sideband events; this uncertainty is estimated from MC simulation to be 0.029% for y_{CP} and 0.007% for A_Γ. Combining the two contributions in quadrature gives total uncertainties of 0.059% for y_{CP} and 0.050% for A_Γ.

Systematics due to the resolution function are estimated using two alternative parameterizations in the fit: one in which the parameter a in Eq. (5) is fixed to zero, and the other in which this parameter is floated but not shared among different decay modes. We find variations of 0.030% for y_{CP} and 0.002% for A_Γ. Systematics due to binning are estimated by varying the number of bins in $\cos\theta^*$ and t. This contribution is found to be 0.021% for y_{CP} and 0.010% for A_Γ.

Possible acceptance variations with decay time are tested by fitting decay time distributions of MC events that pass the selection criteria. We always recover the generated lifetimes, for all decay modes, indicating uniform acceptance. We conclude that this effect is negligible. All individual contributions are added in quadrature to obtain overall systematic uncertainties of 0.09% for y_{CP} and 0.07% for A_Γ.

5. Conclusions

Using the final Belle data set, we measure the difference from unity of the ratio of lifetimes of D^0 mesons decaying to *CP*-even eigenstates K^+K^-, $\pi^+\pi^-$ and to the flavor eigenstate $K^-\pi^+$. Our result is

$$y_{CP} = [+1.11 \pm 0.22\,(\text{stat.}) \pm 0.09\,(\text{syst.})]\% . \qquad (7)$$

The significance of this measurement is 4.7σ when both statistical and systematic uncertainties are combined in quadrature. We also search for *CP* violation, measuring a *CP* asymmetry

$$A_\Gamma = [-0.03 \pm 0.20\,(\text{stat.}) \pm 0.07\,(\text{syst.})]\% . \qquad (8)$$

This value is consistent with zero. These results are significantly more precise than our previous results [4] and supersede them. They are compatible with results from other experiments [8–13] and the world average values [23].

Acknowledgements

References

[1] For a review see: S. Bianco, F.L. Fabbri, D. Benson, I. Bigi, Riv. Nuovo Cimento 26 (7) (2003) 1–200.

[2] S. Bergmann, et al., Phys. Lett. B 486 (2000) 418.

[3] Y. Nir, J. High Energy Phys. 0705 (2007) 102.

[4] M. Starič, et al., Belle Collaboration, Phys. Rev. Lett. 98 (2007) 211803.

[5] B. Aubert, et al., BaBar Collaboration, Phys. Rev. Lett. 98 (2007) 211802.

[6] R. Aaij, et al., LHCb Collaboration, Phys. Rev. Lett. 111 (2013) 251801.

[7] T.A. Aaltonen, et al., CDF Collaboration, Phys. Rev. Lett. 111 (2013) 231802.

[8] J.P. Lees, et al., BaBar Collaboration, Phys. Rev. D 87 (2013) 012004.

[9] T.A. Aaltonen, et al., CDF Collaboration, Phys. Rev. D 90 (2014) 111103(R).

[10] R. Aaij, et al., LHCb Collaboration, Phys. Rev. Lett. 112 (2014) 041801.

[11] R. Aaij, et al., LHCb Collaboration, J. High Energy Phys. 1504 (2015) 043.

[12] R. Aaij, et al., LHCb Collaboration, J. High Energy Phys. 1204 (2012) 129.

[13] M. Ablikim, et al., BESIII Collaboration, Phys. Lett. B 744 (2015) 339.

[14] A. Abashian, et al., Belle Collaboration, Nucl. Instrum. Methods Phys. Res., Sect. A 479 (2002) 117;
Also see detector section in J. Brodzicka, et al., Prog. Theor. Exp. Phys. 2012 (2012) 04D001.

[15] S. Kurokawa, E. Kikutani, Nucl. Instrum. Methods Phys. Res., Sect. A 499 (2003) 1, and other papers included in this volume;
T. Abe, et al., Prog. Theor. Exp. Phys. 2013 (2013) 03A001, and references therein.

[16] Z. Natkaniec, et al., Belle SVD2 Group, Nucl. Instrum. Methods Phys. Res., Sect. A 560 (2006) 1.

[17] E. Nakano, Nucl. Instrum. Methods Phys. Res., Sect. A 494 (2002) 402.

[18] K.A. Olive, et al., Particle Data Group, Chin. Phys. C 38 (2014) 090001.

[19] D.J. Lange, Nucl. Instrum. Methods Phys. Res., Sect. A 462 (2001) 152.

[20] T. Sjostrand, arXiv:hep-ph/9508391.

[21] R. Brun, et al., Technical report CERN-DD-EE-84-1, 1987.

[22] A. Fasso, et al., Conf. Proc. C 9309194 (1993) 493.

[23] http://www.slac.stanford.edu/xorg/hfag/charm/.